J Neurophysiol 113: 3499–3510, 2015.
First published April 8, 2015; doi:10.1152/jn.00051.2015.

CALL FOR PAPERS | *Control of Autonomic Function: Insights from Neurophysiological Studies in Conscious Animals (Including Humans)*

Crossed motor innervation of the base of human tongue

Leszek Kubin,[1] Amy S. Jordan,[1] Christian L. Nicholas,[1] Jennifer M. Cori,[1] John G. Semmler,[2] and John Trinder[1]

[1]*School of Psychological Sciences, University of Melbourne, Melbourne, Australia;* [2]*School of Medical Sciences, University of Adelaide, Adelaide, Australia*

Submitted 20 January 2015; accepted in final form 6 April 2015

Kubin L, Jordan AS, Nicholas CL, Cori JM, Semmler JG, Trinder J. Crossed motor innervation of the base of human tongue. *J Neurophysiol* 113: 3499–3510, 2015. First published April 8, 2015; doi:10.1152/jn.00051.2015.—Muscle fibers of the genioglossus (GG) form the bulk of the muscle mass at the base of the tongue. The motor control of the tongue is critical for vocalization, feeding, and breathing. Our goal was to assess the patterns of motor innervation of GG single motor units (SMUs) in humans. Simultaneous monopolar recordings were obtained from four sites in the base of the tongue bilaterally at two antero-posterior levels from 16 resting, awake, healthy adult males, who wore a face mask with airway pressure and airflow sensors. We analyzed 69 data segments in which at least one lead contained large action potentials generated by an SMU. Such potentials served as triggers for spike-triggered averaging (STA) of signals recorded from the other three sites. Spontaneous activity of the SMUs was classified as inspiratory modulated, expiratory modulated, or tonic. Consistent with the antero-posterior orientation of GG fibers, 44 STAs (77%) recorded ipsilateral to the trigger yielded sharp action potentials with a median amplitude of 52 μV [interquartile range (IQR): 25–190] that were time shifted relative to the trigger by about 1 ms. Notably, 48% of recordings on the side opposite to the trigger also yielded sharp action potentials. Of those, 17 (29%) had a median amplitude of 63 μV (IQR: 39–96), and most were generated by tonic SMUs. Thus a considerable proportion of GG muscle fibers receive a crossed motor innervation. Crossed innervation may help ensure symmetry and stability of tongue position and movements under normal conditions and following injury or degenerative changes affecting the tongue.

genioglossus; hypoglossal nerve; motor units; obstructive sleep apnea; spike-triggered averaging

THE CENTRAL NEURAL CONTROL of the position and shape of the tongue is critical for all oral activities, including vocalization, alimentary functions, and breathing. The tongue can change its shape and produce complex movements because it functions as a hydrostat composed of a complex network of muscle fibers that have no, or only one, rigid point of attachment and are innervated by a large number of hypoglossal (XII) motoneurons exhibiting a wide variety of activity patterns (Fregosi and Ludlow 2014; Kairaitis 2010; Kier and Smith 1985; McClung and Goldberg 2000). Compared with other mammals, humans have a relatively elongated pharyngeal portion of the oral cavity and mobile hyoid apparatus (Fregosi and Ludlow 2014; Lieberman et al. 2001). These two adaptations developed in connection with the evolution of speech, but they have also made the pharyngeal portion of the human upper airway vulnerable to collapse. Airway narrowing and collapse are facilitated by negative intramural pressure during inspiration and can be prevented by activation of the striated muscles surrounding the upper airway, including those forming the base of the tongue (Fregosi 2008; Kezirian et al. 2014; Oliven et al. 2007; Remmers et al. 1978; Sauerland and Harper 1976). Accordingly, in addition to their classic role in alimentary functions and phonation, the muscles of the tongue in humans function as important accessory respiratory muscles and often exhibit prominent inspiratory (I) and tonic (T) activation that helps stiffen the upper airway walls and enlarge the upper airway lumen (Mezanotte et al. 1992; Surat et al. 1988).

The respiratory role of upper airway muscles is particularly important in anatomically predisposed individuals in whom the characteristic sleep-related decline of upper airway muscle activity leads to recurrent inspiratory flow limitation or complete upper airway obstructions, a chronic condition known as the obstructive sleep apnea (OSA) syndrome (Dempsey et al. 2010; Horner et al. 2014; Jordan and White 2008; Patil et al. 2007). OSA is an almost uniquely human disorder that affects about 5% of adults and is associated with arterial hypertension, stroke, excessive daytime sleepiness, and metabolic derangements (Javaheri and Redline 2012; McNicholas and Bonsigore 2007; Newman et al. 2001; Young et al. 2008). Upper airway obstructions are prevented by phasic I and T activation of airway-dilating muscles, including those that form the base of the tongue, because they pull the tongue forward, thereby enlarging the lumen of the upper airway (Kezirian et al. 2014; Oliven et al. 2007). Thus the motor control of the tongue is complex in all mammals and especially so in humans. Perhaps as a consequence of this complexity, there has been relatively little research on the functional anatomy of motor innervation of the human tongue as a whole or its individual muscles. In particular, electrophysiological methods that can importantly extend anatomic findings have not been used to investigate the neuromuscular organization of the human tongue despite its importance for the maintenance of breathing in patients with OSA.

Address for reprint requests and other correspondence: L Kubin, Dept. of Animal Biology 209E/VET, School of Veterinary Medicine, Univ. of Pennsylvania, 3800 Spruce St., Philadelphia, PA 19104-6046 (e-mail: lkubin@vet.upenn.edu).

In recent years, a few studies have described in some detail the gross anatomy of the different muscles of the tongue in humans, including the genioglossus (GG), the largest extrinsic muscle of the tongue, together with the anatomy of their innervation (Abe et al. 2012; Doty et al. 2009; Mu and Sanders 2010; Sanders and Mu 2013; Zur et al. 2004). In humans and other mammals, the GG consists of two compartments, horizontal (GGh) and oblique (GGo) (McClung and Goldberg 2002; Mu and Sanders 2000, 2010). While both compartments are attached to the mandible, the other end of the GGh penetrates into the base of the tongue, whereas the GGo fibers enter the middle sections of the tongue. The GGh muscle fibers have a relatively simple antero-posterior (A-P) orientation, and their contraction mainly pulls the base of the tongue forward. In contrast, the GGo fibers form a fanlike structure and may have either a vertical or transverse orientation, paralleling the vertical and transverse course of the intrinsic tongue muscles. This arrangement results in a dense plexus of contracting elements that generate precise and complex changes in the shape and position of the tongue.

As in other mammals (McClung and Goldberg 2000; Mu and Sanders 1999, 2000), the XII nerve in humans divides into two major branches, lateral and medial, as it enters the tongue along its ventrolateral border. The medial branch provides the motor innervation of the GG. Two or three second-order branches leave the main medial branch and innervate the GGh at motor end-plates (MEP) that distribute medio-laterally along two well-defined bands located within the posterior (closer to the pharynx) half of the muscle (Mu and Sanders 2010) (Fig. 1*A*). Accordingly, action potentials initiated within the GGh may originate from two principal zones from which they propagate in anterior and posterior directions. In contrast, the secondary branches that innervate the GGo are many (up to 50); they branch off from the medial branch of the XII nerve more anteriorly than the branches that innervate the GGh and activate muscle fibers along a single transverse band of MEPs. It is plausible that some motor branches of the hypoglossal nerve innervating the base of the tongue cross the midline and innervate the muscle fibers on the opposite side. However, data from mammals other than humans suggest the absence of crossed motor innervation of the tongue (McClung and Goldberg 2002). In humans, this has not been investigated, but the presence of such an innervation could have important implications for effective functioning of the tongue under both normal and adverse conditions, including a primary injury, as well as OSA, which is associated with strong activation of the muscles of the tongue that may lead to neuromuscular injury (Saboisky et al. 2012; Svanborg 2005).

The anatomical observations reported by Mu and Sanders (2010) can be tested and expanded by electrophysiological techniques. First, the proposal that the base of the tongue comprises only GGh muscle fibers that mainly have an A-P orientation means that it should be possible to record potentials generated by a single motor unit (SMU) using multiple wire electrodes inserted at different levels along the A-P axis on the same side of the midline. Such potentials should occur with an orderly temporal relationship, such that the anterior electrode would typically show a delayed arrival of the action potential relative to the signal recorded by the more posterior electrode because data of Mu and Sanders (2010) show that MEPs are located in the posterior half of the muscle fiber. Second, if neither the muscle fibers nor branches of the motor nerves cross the midline, recordings from the sites located on the opposite sides of the midline should reveal no temporally linked action potentials. Alternatively, the presence or absence of muscle fibers or motor nerves crossing the midline could depend on the functional type of the SMU, a possibility difficult to explore by purely anatomical methods. To investigate these hypotheses, we recorded from left and right and anterior and posterior GG locations and assessed the temporal

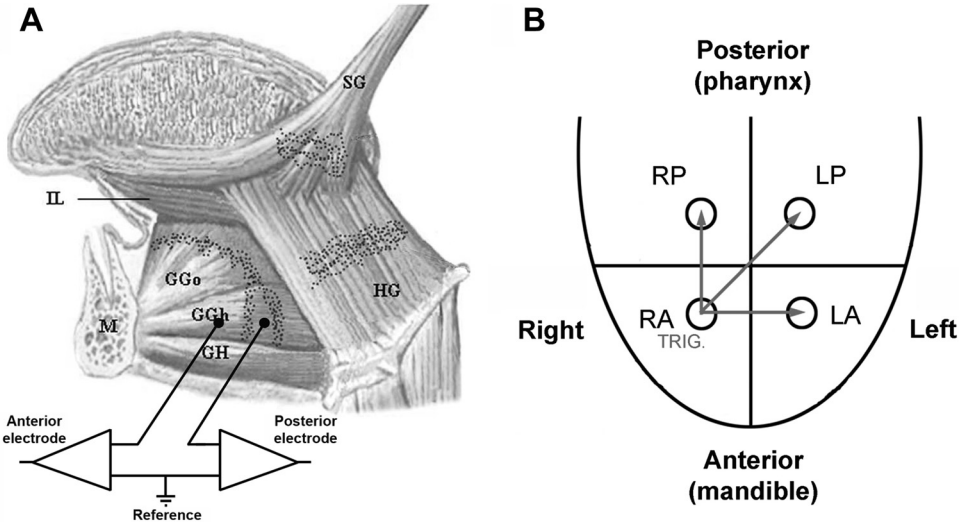

Fig. 1. *A*: schematic representation of the placement of a pair of recording wires on 1 side of the midline, 1 anterior and 1 posterior, within the horizontal compartment of the genioglossus muscle (GGh) of the tongue superimposed on a cross section of major lingual muscles and main locations of motor plates (black dots), as described by Mu and Sanders (2010). GGo, oblique compartment of the genioglossus muscle; GH, geniohyoid muscle; HG, hyoglossus muscle; IL, inferior longitudinal muscle; M, mandible; SG, styloglossus muscle. Background image reproduced with permission from Wiley-Liss publishers and authors. *B*: antero-posterior (A-P) and medio-lateral positions of the 4 recording wires placed in the GGh muscle and the nomenclature used to describe each of the 4 recording leads. In this example, the trigger motor unit (TRIG.) is recorded with the right anterior (RA) electrode. As a consequence, the right posterior (RP) is the ipsilateral electrode, left anterior (LA) is the contralateral electrode placed at the same A-P level as the trigger, and left posterior (LP) is the contralateral electrode located at A-P level other than the trigger.

relationship between potentials recorded at different sites using the technique of spike-triggered averaging (STA). Our results corroborate the anatomical information about the neuromuscular organization of the base of the tongue in humans and provide compelling evidence of a crossed motor innervation that unevenly involves different classes of SMUs. A preliminary report has been published (Kubin et al. 2014).

METHODS

Subjects. The subjects were 16 males with a mean age of 28.6 ± 12.4 yr (SD), a mean height of 178 ± 6 cm, and a mean weight of 76 ± 13 kg. The data collection protocol included exposing the subjects to hypercapnia and inspiratory loads; the results from the hypercapnic trials have since been published (Nicholas et al. 2010). As elevated CO_2 may affect the fetus and pregnancy testing was not available, women were excluded from the study. All subjects were healthy and reported no sleep or respiratory complaints, as determined by a questionnaire. The protocol conformed to the Declaration of Helsinki and had prior approval of the local Human Subjects Ethics Committee of the University of Melbourne. Informed, written consent was obtained from each subject.

Subject instrumentation and data collection procedures. All recordings were conducted during the late morning or early afternoon. Subjects were requested to refrain from alcohol for 24 h and from food and caffeine for 4 h before the experiment. Upon each subject's arrival at the laboratory, an anesthetic cream was applied under the subject's chin (Lidocaine-Prilocaine; Fogera, Melville, NY). Instrumentation of the subject commenced 30 min later.

For monitoring of airway pressure, a catheter containing a pressure transducer was inserted via a nostril and positioned at the level of the epiglottis (MPC-500; Millar, Houston, TX). The subjects wore a full face mask (type 431; Fisher and Paykel, Auckland, NZ) equipped with a two-way breathing valve (type 2600-medium; Hans Ruddolph, Shawnee, KS), a pneumotachometer (type 3719, Hans Ruddolph), a differential pressure transducer (DP-45; Validyne, Northridge, CA), a CO_2 analyzer (CD-3A; Ametek, Berwyn, PA), and an oxygen analyzer (S-3A/I; Ametek). The signals from these transducers were amplified, low-pass filtered at 15 Hz (Grass Telefactor Amplifiers, Warwick, RI) and digitized at 100 Hz using a 1401 interface and Spike-2 acquisition software (Cambridge Electronic Design, Cambridge, UK).

The procedures used to record electromyogram (EMG) followed those of Eastwood et al. (2003). Four wire electrodes were made of a single-stranded, 50-μm-thick, stainless steel and Teflon-coated wire (A-M Systems, Seattle, WA). The wires, with insulation removed over 0.5 mm at the tip, were inserted into the base of the tongue through the skin of the chin to a depth of 2.4 cm using a 25-G hypodermic needle. Previous ultrasonic measurements indicated that wire electrodes inserted to this depth were consistently positioned within the GG muscle (Eastwood et al. 2003; Saboisky et al. 2006; Wilkinson et al. 2008). In each subject, four wires were inserted, two at ~3 mm to the left and right from the midline at the level located ~10 mm from the inferior margin of the mandible and another two at ~3 mm to the left and right from the midline at a level ~20 mm from the inferior margin of the mandible (Fig. 1*B*). EMG signals recorded at each site were referenced to a common surface electrode positioned over the bony mandible. They were filtered at 0.03–3.0 kHz, digitized at 10 kHz, and acquired using the same 1401 interface and Spike-2 software.

During data collection, the subjects lay supine on a bed in a dimly illuminated room. The supine position was used, as it is an easy position to standardize and maintain and because it tends to enhance GG activity (Malhotra et al. 2004). Subjects were instructed to remain still and relaxed, relax facial muscles, try to avoid swallowing, and remain awake. They initially breathed room air for 5 min to become accustomed to breathing through the face mask. They were then subjected to six CO_2 trials with an elevation of $P_{ET_{CO_2}}$ to 8.4 ± 2.0 mmHg above their baseline and eight trials in which a resistor (5, 10, 15, or 20 $cmH_2O \cdot l^{-1} \cdot s^{-1}$) was placed in the inspiratory line. Each trial lasted up to 3 min, including a 30-s baseline. At all other times, subjects remained quietly awake in the supine position and breathed room air.

Selection of data for analysis. The data segments targeted for analysis were selected from the periods between hypercapnic or respiratory load trials at times when breathing was stable, as determined by a steady breath-to-breath tidal volume. The four lingual EMG traces were inspected for epochs during which a spike train possibly generated by an SMU was clearly distinguishable in at least one of the four EMG recordings. The amplitude of the spikes in such a recording had to be sufficiently large to allow for reliable spike discrimination using a threshold voltage-crossing routine included in the Spike-2 software. Interspike interval histograms were generated to verify that the train used for triggering had the absolute refractory period and unimodal distribution consistent with its origin in an SMU. Each spike train that fulfilled these criteria was then designated to be used as the source of triggers for that epoch. The exclusion criteria for an epoch to be considered for analysis were body movements or overt respiratory or state instability that would make the signals nonstationary. With these criteria fulfilled, the durations of separate epochs were determined by the available periods of stable activity of the SMUs used as triggers. The durations of the analyzed epochs varied from several seconds to several minutes and contained 45-2,362 triggering spikes (mean: 488 ± 345) generated at average discharge rates of 9–31 Hz (mean: 17.8 ± 4.0 Hz). In each subject, a particular SMU was used as trigger only once.

Motor unit classification and generation of spike-triggered averages. Activity of human GG motor units has been classified into different patterns relative to the phase of the respiratory cycle (e.g., Bailey 2011; Saboisky et al. 2006). In the present study, to categorize the discharge patterns of the studied SMUs, standard pulse trains obtained from spike discrimination were converted to plots of instantaneous firing rate, and the position of the peak of firing rate with respect to the time course of the airflow and epiglottic pressure signals was visually determined. The five categories of SMUs identified were as follows: *1*) inspiratory phasic (IP), when the peak firing rate occurred during inspiration, and the lowest rate was <2.0 Hz (i.e., the unit was silent for at least 500 ms); *2*) inspiratory tonic (IT), when peak activity occurred during inspiration and was >2.0 Hz throughout the respiratory cycle; *3*) expiratory phasic (EP), when the peak firing rate occurred during expiration, and the lowest rate was <2.0 Hz; *4*) expiratory tonic (ET), when peak activity occurred during expiration and was >2.0 Hz throughout the respiratory cycle; and *5*) T, when the units fired at a steady rate throughout the respiratory cycle.

Once a reliable source of triggering action potentials originating in an SMU was identified, STA was used to detect potentials temporarily related to the occurrence of the triggering potential at the other three recording sites. The technique is analogous to averaging of potentials evoked by an external stimulus to determine whether electrophysiological activity at the recording site is temporally related to the trigger. When there is no such relationship (i.e., recorded signal is random relative to the trigger), the evoked response averages to zero. The technique has been previously used to investigate neuromuscular organization in humans (e.g., Disselhorst-Klug et al. 1999; Masuda and De Luca 1991; Monster and Chan 1980). The selection of the trace that provided triggers for STA was entirely dictated by the presence of an SMU signal with action potentials suitable for automatic detection with the Spike-2 software. Once the trigger source was defined, one of the remaining three traces would consequently become the one recorded ipsilaterally to the trigger, and the other two would be recorded from sites located contralateral to the trigger. Distinction was also made between triggers derived from the recording sites located at the anterior and posterior levels. Accordingly, an ipsilateral STA could be obtained from a site located either anterior or

posterior to the trigger depending on the locations of the trigger and the recording site. Similarly, the contralaterally recorded STAs could be recorded at the same A-P level as the trigger or at the site located diagonally to the trigger (i.e., at the other A-P level; Fig. 1*B*). STAs were generated using Spike 2 software, with the time scale covering the period from 5 ms before to 20 ms after the triggering spike.

The STA potentials obtained from each recording site were examined for the presence of triphasic potentials having a similar configuration and similar duration (1–4 ms) to those of the triggering potentials. This, together with a tight temporal relationship of the STA potentials to the trigger, indicated that they were generated in the muscle fibers that were a part of the same SMU as the trigger even though they were recorded at a different location in the base of the tongue from that of the trigger.

The amplitudes of trigger potentials and STA potentials were measured as the difference between the potentials' positive and negative peaks (peak-to-peak), and the latency of the STA potentials was measured between the main negative peak of the triggering potential and the main negative peak of the STA potential. We empirically determined that, when STA traces contained a distinct triphasic potential with an amplitude at least twice the amplitude of the noise present across the entire average trace, this could be considered with high probability indicative of the presence of muscle fiber(s) belonging to the studied SMU in the proximity of a given recording wire. The trials yielding the average potentials that fulfilled these criteria were classified as positive STA trials. Conversely, when an STA trace contained no distinct triphasic potential with an amplitude at least twice the amplitude of the noise, this was taken as indicative of the absence of any muscle fiber belonging to the studied SMU being present in the vicinity of a given recording wire, and the STA trial was deemed negative.

The STA potentials could precede the trigger (negative latency, or a lead, relative to the trigger), coincide with the trigger (zero latency), or follow the trigger (positive latency, or a lag, relative to the trigger). The STA potentials that were distinctly time shifted relative to the triggering potential by more than ± 0.1 ms (resolution of our latency measurements) were assumed to originate in muscle fibers of the same SMU as the trigger but transmitted to another location along the motor nerve branches and/or muscle membrane. The zero latency potentials were distinguished because they could represent an electrotonic spread of the action potential from the trigger-recording site, rather than a genuine case of propagation of the action potential in the motor nerve terminal branches and/or the muscle fibers. Accordingly, all STA potentials whose peaks coincided with the peak of triggering potential, or were time shifted by not more than ± 0.1 ms, were classified as zero latency potentials. Theoretically, a few zero latency potentials recorded on the same side as the trigger could be falsely classified as resulting from electrotonic spread if the trigger and the averaged signals were located such that the MEP was midway between them because the STA potential would then theoretically arrive at approximately the same time to both recording electrodes, resulting in zero latency. However, in reality, zero latency occurred in only 3 out of 47 STAs containing a distinct potential ipsilaterally to the trigger. On the side opposite to the trigger, zero latency potentials were detected more frequently (14 out of 73 STAs containing a distinct potential), but their mean amplitudes were very low compared with the amplitudes of contralaterally recorded STA potentials with nonzero latencies (see RESULTS). This amplitude difference supported the interpretation that the zero latency potentials registered contralateral to the trigger occurred as a result of electrotonic spread from the opposite side. To minimize any confounding effect of zero latency potentials on our conclusions, such potentials recorded on either side relative to the trigger were distinguished as a separate category.

Statistical analysis. The incidence of distinct STA potentials was analyzed as a function of the signal origin relative to the trigger location and in relation to the discharge pattern of the triggering motor unit using χ^2 statistics with Yates correction for continuity. Normality of the distributions was tested using the Shapiro-Wilk test. The amplitudes and durations of triggering potentials and STA potentials, and the STA potential latencies in relation to the recording location vs. trigger location and SMU discharge pattern, were analyzed using one-way ANOVA with Holm-Sidak correction for multiple comparisons when data were normally distributed and using Kruskal-Wallis one-way ANOVA on ranks with Dunn correction when data sets were not normally distributed. Any subsequent post hoc comparisons were conducted using unpaired, two-tailed Student's *t*-test and Mann-Whitney rank sum test, respectively. The extent to which the amplitudes of potentials simultaneously obtained from different sites, or amplitudes and durations of potentials recorded from the same site, were correlated was assessed using Spearman correlation. SigmaPlot v. 12.8 (San Jose, CA) was used for all statistical analyses. Variability of the measurements is characterized by the means $\pm$ SD or by the median and 25–75% interquartile range (IQR) for normally distributed and not normally distributed data sets, respectively.

RESULTS

Incidence of STA potentials. Sixty-nine data epochs meeting the inclusion criteria were identified and analyzed in 16 recordings from 16 subjects (range: 1–9 epochs with different SMUs used as triggers per subject). Of the 69 epochs, 30 used triggers recorded with an anterior electrode and 39 with a posterior electrode. The 69 epochs could potentially yield 207 STAs should all the remaining three recording signals in all subjects be of satisfactory quality: 69 ipsilateral, 69 contralateral at the same A-P level, and 69 contralateral at the A-P level different from the trigger. However, signals from 26 recording sites were discarded because of their poor technical quality (12 ipsilateral and 14 contralateral, to the trigger), resulting in 181 technically valid recordings that could have yielded distinct STA potentials. Of those, 103 STAs contained genuine average potentials that were time shifted relative to the trigger. Of the remaining 78 technically valid recordings, 17 yielded zero latency potentials, and 61 did not result in an identifiable potential (negative STA trials). Table 1 provides information about the incidence of positive and negative STA trials in relation to different combinations of the triggering and recording sites.

The most important finding from the analysis of the incidence of STA potentials was that, although distinct STA potentials with nonzero latency were significantly more likely to occur at the recording sites located ipsilateral to the trigger (77%) than contralaterally (48%), contralateral potentials occurred in almost half of the tested trigger-recording site combinations, with the difference between the two proportions being significant [$\chi^2(1) = 12.1$, $P = 0.0005$]. For the STAs between the signals recorded on the same side of the midline, the incidence of positive STAs for triggers located anteriorly and averaged potentials derived from posterior locations was not different from that for the opposite arrangement in which the trigger was located posteriorly and recording was from the anterior site (82% vs. 72%; Table 1).

Figure 2*A* shows a typical example of STA potentials obtained ipsilaterally and contralaterally to the triggering potential with an SMU used for triggering that had IP type of activity. In this case, the STA potential obtained from the site located on the same side as the trigger and posterior to it preceded the trigger by 0.6 ms and had peak-to-peak amplitude of over 150 μV. Both STA potentials recorded contralaterally

Table 1. *Numbers of STA trials and percentage of occurrence of positive, zero latency, and negative STAs in relation to the location of the trigger and recording site*

	Ipsilateral STAs		Contralateral STAs			
			Anterior Triggers		Posterior Triggers	
	Anterior Triggers	Posterior Triggers	Posterior STAs	Anterior STAs	Posterior STAs	Anterior STAs
No. of trigger SMUs tested	28	29	24	28	35	37
Positive STAs	23 (82%)	21 (72%)	11 (46%)	14 (50%)	19 (51%)	15 (41%)
Zero latency STAs	1	2	2	5	6	1
Negative STAs	4	6	11	9	10	21

Positive spike-triggered average (STAs), STA trials that yielded distinct potentials with nonzero latency relative to the trigger; zero latency STAs, STA trials that yielded distinct potentials with <0.1 ms time shift (lead or lag) relative to the trigger; negative STAs, STA trials with no distinct potential having a configuration compatible with a single motor unit (SMU) action potential or with amplitude not exceeding twice the noise level in the average trace.

to the trigger were delayed by about 2 ms from the trigger and had amplitudes in 25–60 μV range.

The zero latency STA potentials were distinguished as a separate category because they could represent electrotonically spreading field potentials, rather than a genuine membrane transmission of action potentials from one site to another (see METHODS). When STA was conducted across the midline, zero latency potentials occurred in 11.3% of the trials, and, when both the trigger and the recording site were located on the same side, they occurred in 5.3% of trials (the difference was not significant; Table 1). For the zero latency potentials recorded on the opposite side to the trigger, their incidence tended to be higher in the trials in which both the trigger and the recording site were at the same level (anterior or posterior; 17.4%) than when the trigger and the recording sites were positioned diagonally against each other, i.e., anterior trigger and posterior recording site on the opposite side or posterior trigger and anterior recording on the opposite side [4.9%; $\chi^2(1) = 3.7$, $P = 0.055$]. This was consistent with the hypothesized electrotonic nature of the spread of these potentials.

Trigger and STA potential amplitudes and durations. Amplitudes of the potentials varied with their origin and nature. Expectedly, the trigger potentials (median: 311 μV, IQR: 205–492, $n = 69$) were significantly larger than the nonzero latency STA potentials recorded on the same side as the trigger (52 μV, IQR: 25–190, $n = 44$; $P < 10^{-13}$, rank sum test). In this analysis, trials that did not yield any distinct STA potentials were excluded, but entering zero values for negative STA trials yielded similar statistical outcomes. The difference between the trigger potentials and STA potentials reflected the prior selection of the motor units for use as triggers based on the amplitudes being sufficiently large for a reliable automatic recognition of their action potentials. There was no difference between the amplitudes of the contralateral nonzero latency potentials recorded at the same level as the trigger (median: 17 μV, IQR: 11–44, $n = 33$) and those recorded at the other level

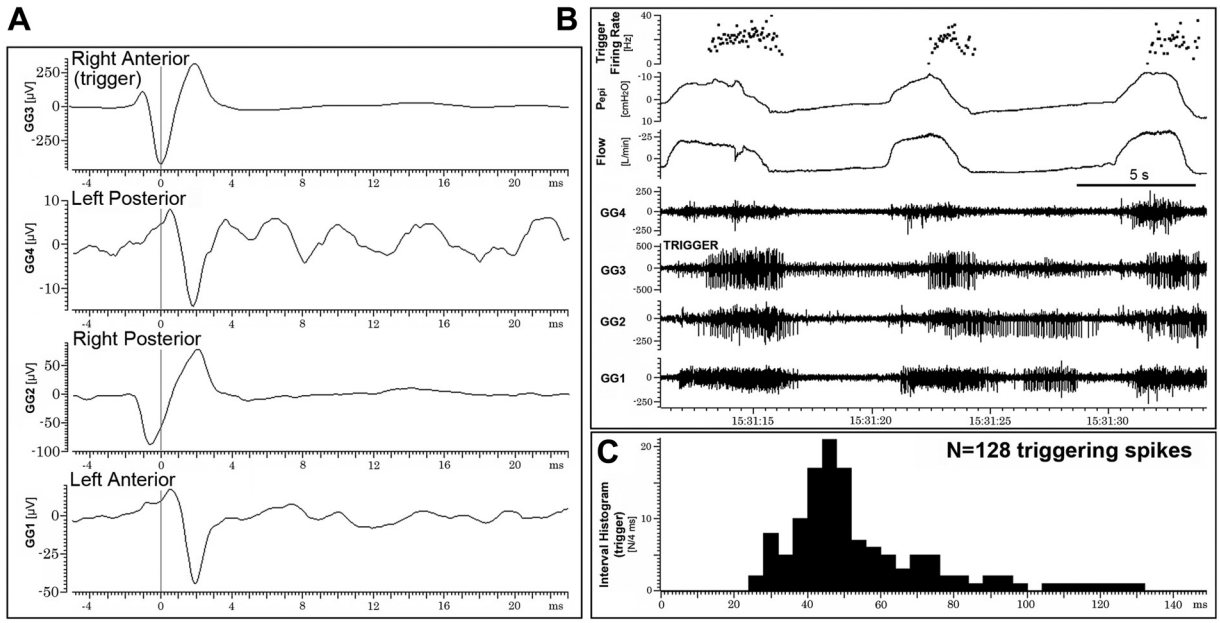

Fig. 2. Example of spike-triggered averaging (STA) potentials obtained with a motor unit having a late inspiratory phasic (IP) activity pattern. *A*: average triggering potential (RA recording site labeled GG3) and the 3 STA potentials; the ipsilateral (RP, GG2) and the 2 contralateral potentials (LA, same level, GG1; and LP, different level, GG4). *B*: polygraphic traces for the motor unit used to obtain the average potentials shown in *A*. From top, the instantaneous frequency of action potentials on the trigger electrode, epiglottic pressure, mask airflow, and the 4 raw electromyogram signals with the second from top (GG3) labeled as the one used to trigger the averaging. *C*: interspike interval histogram for the triggering action potentials has a unimodal distribution and prolonged refractory period, as expected of a train of action potentials generated by a single motor unit. The histogram is based on the same segment of record as that used to generate the average traces shown in *A*.

(19 μV, IQR: 13–28, $n = 26$; $P = 0.96$, rank sum test). All contralateral STA potentials combined were significantly smaller than the STA potentials recorded on the same side as the trigger (18 μV, IQR: 12–36, $n = 59$; $P < 10^{-11}$). They were, however, significantly larger than the zero latency STA potentials recorded contralateral to the trigger (11.6 μV, IQR: 3.1–16.0, $n = 14$; $P = 0.005$). The particularly small amplitudes of the zero latency potentials was consistent with them representing electrotonic spread of field potentials generated at a distance from the recording site (i.e., on the opposite side of the midline). Table 2 lists the amplitudes and latencies for different subgroups of STA potentials defined by the relative positions of the trigger and STA recording site and the lead or lag of the STA potential relative to the trigger.

Figure 3*A* shows the distribution of amplitudes of the trigger potentials and all STA potentials of different categories. It is of note that, among the 59 contralateral STAs with nonzero latencies, 17 (28.8%) had amplitudes above 30 μV (median: 63 μV, IQR: 39–96). This was higher than any of the zero latency potentials, and the range of amplitudes for these 17 potentials overlapped with the range of amplitudes for ipsilateral STAs with nonzero latencies. Thus at least these 17 contralateral STAs must have been generated in muscle fibers located close to the recording site and, therefore, within the base of the tongue on the side opposite to the trigger.

Spearman correlations were computed to determine whether the amplitudes of trigger potentials were related to the amplitudes of their associated STA potentials. There was a significant positive correlation between the anterior trigger potentials and the ipsilateral posterior STAs [$r(22) = 0.48$, $P = 0.02$], but the correlation between the posterior trigger potentials and ipsilaterally located anterior STAs was not significant [$r(20) = 0.17$, $P = 0.45$]. There was a positive correlation between the trigger potentials and the contralateral STAs recorded at the same level as the trigger [$r(32) = 0.44$, $P = 0.01$] but not between the amplitudes of trigger potentials and the STA potentials obtained from the level different from that of the trigger (e.g., anterior trigger and contralateral posterior STA) [$r(25) = -0.14$, $P = 0.47$]. There was also a strong positive correlation between the amplitudes of the anterior and posterior contralateral STAs irrespective of the anterior or posterior location of the trigger [$r(19) = 0.77$, $P = 0.2 \times 10^{-5}$].

As with amplitudes, the durations of the trigger and STA potentials varied with the potential's type and recording site (Fig. 3*B*). The trigger potentials were of significantly shorter duration than any subset of nonzero latency STA potentials. The medians/IQRs were as follows: 1.8 ms/1.3–2.2 for the triggers ($n = 69$), 2.5 ms/1.8–3.3 for the STAs recorded ipsilaterally ($n = 44$), and 2.5 ms/1.8–3.0 for the STAs recorded contralaterally ($n = 59$), with the origin of the potential being a significant factor for differences among the groups ($P = 0.001$, 1-way ANOVA on ranks). The contralaterally recorded STA potentials with zero latencies (median: 1.15 ms, IQR: 0.45–3.2, $n = 14$) were significantly shorter than the durations of nonzero latency STA potentials recorded either ipsilaterally ($P = 0.03$, $n = 44$) or contralaterally ($P = 0.02$, $n = 59$) to the trigger. Thus, consistent with the amplitude data, the particularly short durations of the zero latency potentials pointed to these potentials being caused by electrotonic spread from a source located at a distance from the recording site, as this would occur without a temporal dispersion of the potential that occurs when the potential is transmitted by membrane conduction.

STA potential latencies. As indicated in METHODS, STA potentials could either precede (negative latency) or follow (positive latency) the trigger potential. Table 2 shows the distributions of STAs with negative and positive latencies in relation to the position of the trigger and the recording site. For ipsilateral STAs, when the trigger electrode was in an anterior location, the ipsilateral STA (posterior electrode) typically preceded the trigger potential (19 of 23 trials, or 82%). Conversely, when the trigger electrode was in a posterior location, the ipsilateral STA (anterior electrode) was less likely to have a negative latency with respect to the trigger potential (preceding the trigger potential in 9 of 21 trials, or 43%). Thus, in 70% of trials (31 of 44), the potential on the posterior electrode, whether it was a trigger or STA, preceded the potential on the anterior electrode, the percentage being nearly significantly different from a random 22:22 distribution [$\chi^2(1) = 3.0$, $P = 0.08$].

In contrast to the ipsilateral STAs, the direction of latencies for the contralateral STAs did not systematically vary as a function of A-P location of the trigger. Rather, as indicated in Table 2, most (46 out of 59, or 78%) of the contralateral

Table 2. *Median amplitudes with IQRs and the mean latencies with SD of STAs in relation to the location of the trigger and recording site*

	STAs with Leads Relative to Trigger			STAs with Lags Relative Trigger		
	Amplitude [μV]	Latency [ms]	n	Amplitude [μV]	Latency [ms]	n
Recordings ipsilateral to trigger						
Posterior triggers	54, IQR: 31–237	−1.1 ± 0.9	9	23, IQR: 12–68	1.0 ± 0.9	12
Anterior triggers	67, IQR: 41–168	−1.1 ± 0.6	19	147, IQR: 65–294	0.9 ± 0.6	4
Recordings contralateral to anterior triggers						
Posterior STA (other level than trigger)	85, IQR: 6–89	−4.3 ± 1.6	3	19, IQR: 14–21	2.9 ± 1.3	8
Anterior STA (same level as trigger)	87, IQR: 34–117	−3.45 ± 2.6	4	23, IQR: 9–63	2.3 ± 1.6	10
Both anterior and posterior STAs	85, IQR: 10–116	−3.8 ± 2.1	7	19, IQR: 12–29	2.7 ± 1.5	18
Recordings contralateral to posterior triggers						
Posterior STA (same level as trigger)	12, IQR: 10–19	−2.15 ± 1.1	4	16, IQR: 12–36	3.7 ± 1.9	15
Anterior STA (other level than trigger)	5.2–13.5	−0.6 ± −1.40	2	23, IQR: 14–31	2.8 ± 1.9	13
Both anterior and posterior STAs	12, IQR: 9–13	−1.8 ± 1.1	6	17*, IQR: 13–35	3.3 ± 1.9	28

Negative and positive latencies correspond to the cases when STAs preceded (lead) and lagged the trigger, respectively. *$P = 0.04$ relative to STAs with leads (rank sum test); n, number of SMUs tested. IQR, interquartile range.

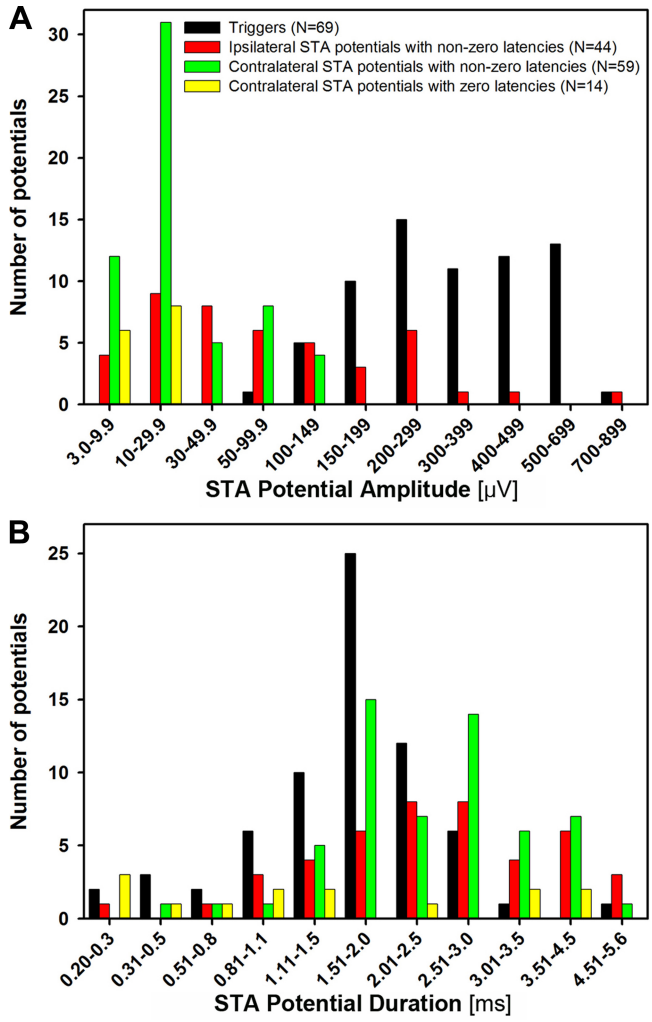

Fig. 3. Distribution of the amplitudes of all trigger action potentials and all STA potentials recorded from up to 4 sites within the GGh compartment of the tongue in all subjects (*A*) and the corresponding data for the durations of these potentials (*B*). See text for a detailed comparison of the amplitudes and durations of different categories of STA potentials.

potentials followed the trigger potential, this being a significant bias compared with a random distribution [$\chi^2(1) = 8.9$, $P = 0.003$].

STA potential characteristics in relation to the motor unit discharge pattern. The incidence, amplitudes, and durations of STA potentials were investigated as a function of the discharge characteristics of the studied SMUs. Of the 69 triggers, 13 were of IP, 13 of IT, 2 of EP, 28 of ET, and 12 of T type (Fig. 4*A*). One additional unit had variable discharge with a pattern that was not related to the respiratory cycle. As previous studies have shown that inspiratory-modulated (IP and IT) motor units have many similarities, as do expiratory-modulated (EP and ET) units (Nicholas et al. 2010; Wilkinson et al. 2008, 2010), these subgroups were combined, resulting in 26 I, 30 expiratory (E), and 12 T motor units, whereas the one nontonic, nonrespiratory unit was excluded from further analysis. Mean firing rates were calculated within the main three functionally distinct groups of SMUs, but no differences were detected. The mean firing rate for all SMUs regardless of their firing pattern was 17.8 ± 4.0 Hz, and the within-group (unit type) means varied between 15.7 and 19.0 Hz.

The incidence of distinct, nonzero latency ipsilateral and contralateral STA potentials as a function of SMU discharge pattern is illustrated in Fig. 4*B*. For both I and E units, the probability of detecting an STA potential on the same side as the trigger was significantly higher than on the side opposite to the trigger [71.4% vs. 36.0% for I units; $\chi^2(1) = 5.90$, $P = 0.015$; and 88.0% vs. 55.7% for E units; $\chi^2(1) = 6.47$, $P = 0.011$]. In contrast, for T units, this difference was not significant [63.6% vs. 54.5%; $\chi^2(1) = 0.24$, $P = 0.62$]. Thus only for the T units the probability of obtaining an STA potential contralaterally to the trigger did not significantly decline compared with the STAs conducted ipsilateral to the trigger.

The amplitudes of STA potentials also differed as a function of the SMU discharge pattern (Fig. 4*C*). A two-by-three ANOVA (ipsilateral vs. contralateral location, and I vs. E vs. T discharge pattern), in which only STA potentials with nonzero latencies were included, indicated both a significant effect of the location of the recording site [$F(1,96) = 8.37$, $P = 0.0047$] and a significant interaction between the SMU activity pattern and recording location [$F(2,96) = 4.08$, $P = 0.02$]. The recording location effect was due to the significant difference between the amplitudes of STA potentials recorded ipsilateral and contralateral to the trigger, as described earlier. Subsequent analysis of this issue in relation to the SMU firing pattern revealed that ipsilateral STA potentials were larger than contralateral potentials for I units (median: 111.2 μV, IQR: 42.7–232.5, $n = 15$ vs. 12.8 μV, IRQ: 8.2–19.3, $n = 17$; $P = 0.001$), and the same was the case for the E units (median: 43.4 μV, IQR: 25.5–197.7, $n = 22$ vs. 17.6 μV, IQR: 12.6–29.1, $n = 29$; $P = 0.1 \times 10^{-11}$). In contrast, ipsilateral and contralateral STA potential amplitudes did not differ for the T units, with the median STA potentials recorded contralateral to the trigger being slightly larger than for the ipsilateral ones (40.3 μV, IQR: 15.0–55.9, $n = 7$ vs. 83.1 μV, IQR: 26.4–116.3, $n = 11$; $P = 0.17$). Compared with contralateral STA potentials for the T units, the amplitudes of contralateral STA potentials for either I or E units were very small and significantly smaller ($P = 0.1 \times 10^{-11}$ for both) (Fig. 4*C*). Furthermore, the incidence of contralateral STA potentials >30 μV relative to all contralateral recordings tested was minimal for I units (4/47, or 4.3%), somewhat larger for E units (8/52, or 15.3%), and largest for the T units (7/23, 30.4%), with the difference between the I and T units being significant [$\chi^2(1) = 7.25$, $P = 0.007$]. Thus the picture that emerged from this analysis was that T units were the main ones yielding contralateral potentials with both a high probability and large amplitudes. T units were followed in this regard by the E units, whereas for I units the probability of occurrence of contralateral potentials of relatively large amplitude was lowest. Figure 5 shows an example of STA potentials obtained with a T unit that characteristically produced a relatively small STA potential on the same side as the trigger (40 μV) and relatively large and wide potentials at both contralateral sites (89–119 μV).

Analysis of STA potential durations relative to the SMU firing patterns yielded one significant result consistent with relatively small contribution of I units to contralateral STA potentials. Specifically, the contralateral STA potentials obtained from I units had significantly shorter durations than contralateral STA potentials obtained with either E or T units (Fig. 4*D*).

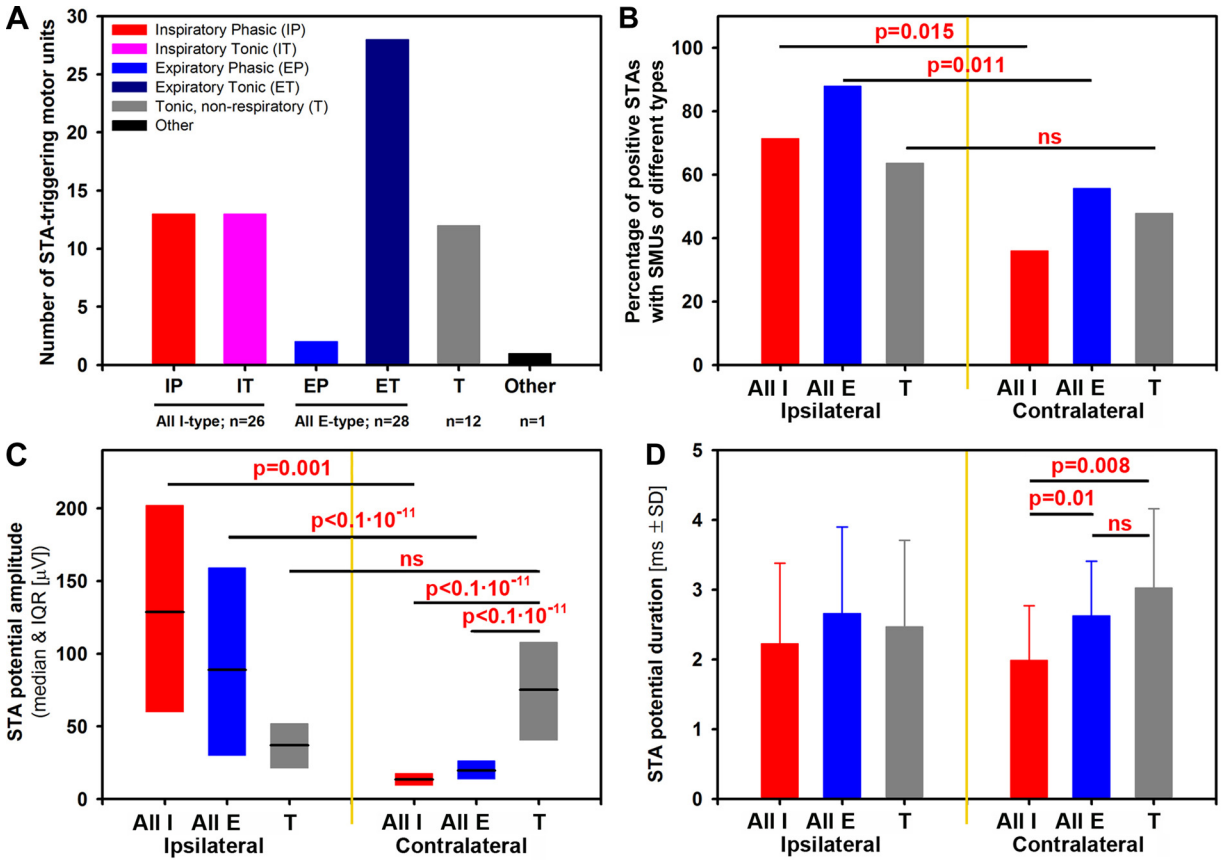

Fig. 4. Properties of STA potentials in relation to the single motor unit (SMU) discharge pattern. *A*: distribution of the numbers of studied SMUs with different activity patterns. *B*: percentage of positive STA potentials obtained with SMUs having different activity patterns. *C*: median amplitudes and interquartile ranges (IQR) of the STA potentials recorded ipsilateral and contralateral to the trigger for SMUs with different activity patterns. *D*: durations of ipsilateral and contralateral STA potentials for SMUs with different activity patterns. Based primarily on the amplitude distribution (*C*), tonic (T) muscle fibers received most prominent crossed motor innervation. E, expiratory; I, inspiratory.

DISCUSSION

Consistent with a predominantly longitudinal orientation in the A-P direction of the muscle fibers comprising the base of the tongue, we found relatively large and frequent STA potentials at the recording sites located on the same side of the midline and either anterior or posterior to the position of the trigger potential. Indeed, the amplitudes of such potentials were almost one-third the amplitudes of the trigger potentials, with the latter having been selected on the basis of being particularly large and obviously above any background activity. Furthermore, the time shifts between ipsilaterally recorded potentials were such that the potentials on the anterior electrode, whether the trigger or STA potential, were in most cases delayed with respect to potentials on posterior electrodes. This is consistent with action potentials being predominantly transmitted along the muscle fiber membrane primarily in the A-P orientation from posterior sites, where most motor end plates are located, to more anterior levels, where GG muscle fibers are attached to the mandible. The typical time shift between ipsilaterally recorded trigger potentials and STA potentials was of the order of 1 ms over a distance of 1 cm, which is compatible with a conduction velocity of 7–10 m/s measured for action potential transmission in muscle fibers of skeletal muscles (Arendt-Nielsen and Zwarts 1989). Thus our STA data obtained with both the trigger and recording site located on the same side of the midline are consistent with the notion that most muscle fibers comprising the base of the tongue form bands that run in an A-P orientation. Furthermore, given that our posterior recording wire was placed ~2 cm posterior to the mandible, the pattern where most posteriorly recorded potentials preceded those recorded at the anterior sites also is compatible with the predominant position of the motor plates in the GGh, as described by Mu and Sanders (2010) on the basis of their anatomical study (Fig. 1*A*).

In addition to obtaining electrophysiological data consistent with the prior anatomical evidence for longitudinal organization of muscle fibers in the base of the human tongue, we obtained compelling evidence that supports the presence of a previously unreported crossed motor innervation of the human tongue and the evidence that such a crossed innervation is particularly common in the case of T motor units. In the following, we will concentrate on these novel findings.

Evidence for crossed motor innervation of muscle fibers in the base of the human tongue. Animal studies have suggested that crossed inputs are transmitted to the motor systems controlling the tongue at central premotor levels and through midline-crossing dendrites of XII motoneurons, whereas the peripheral projections of motor axons do not cross the midline at the muscle level (Altschuler et al. 1994; McClung and Goldberg 2000, 2002; Peever and Duffin 2001; Tarras-Wahlberg et al. 2009). Similarly, Mu and Sanders (2010) did not note motor axonal branches that crossed the midline in their

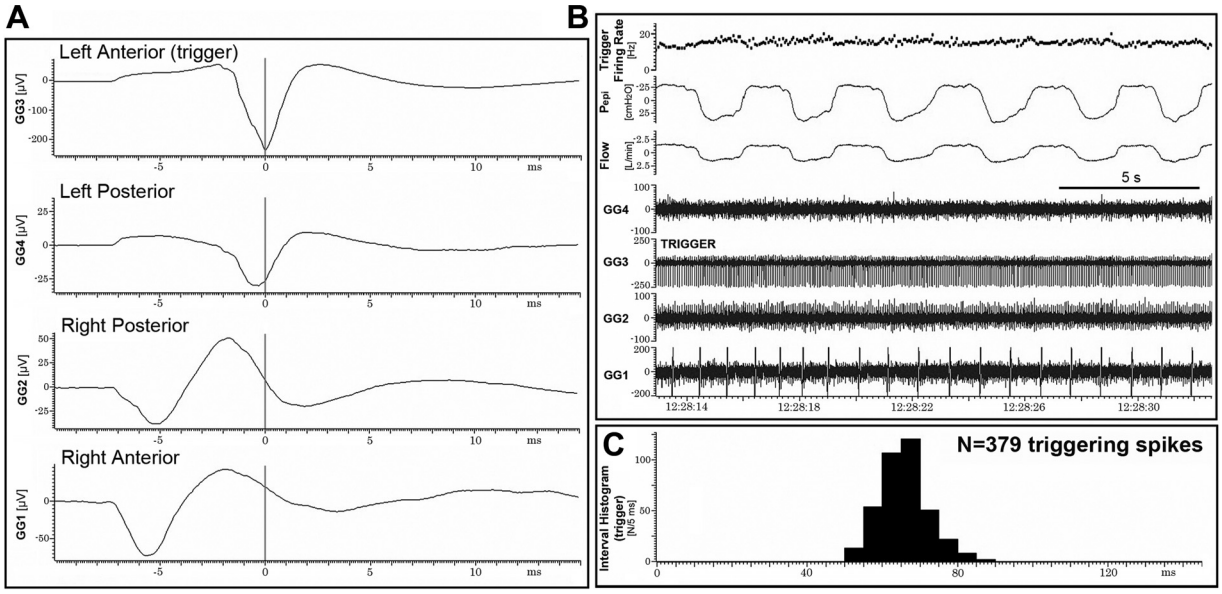

Fig. 5. Example of STA potentials obtained with a motor unit with T activity pattern. *A*: characteristically for T motor units, the unit had a relatively small STA potential on the same side as the trigger (40 μV, second from top trace in *A* labeled GG4) and relatively large and broad STA potentials at both contralateral sites (89–116 μV, 2 bottom traces in *A* labeled GG2 and GG1). These large contralateral STA potentials precede the trigger (GG3 in *A*), suggesting that this motor unit received its motor innervation from the right hypoglossal nerve. The design of *B* and *C* is the same as in Fig. 2. The bottom trace in *B* labeled GG1 includes relatively prominent ECG artifacts, but their presence did not adversely affect the averaging, as indicated by similarly smooth STA potentials in both GG2 and GG1 in *A*.

study of the human tongue, but, admittedly, such branches would be difficult to identify in a conclusive manner in their material. Important for our considerations here is to note that the evidence that muscle fibers comprising the base of the tongue do not cross the midline is rather compelling, as this would have been readily identified by Mu and Sanders (2010) and Sanders and Mu (2013). In contrast, the absence of data for motor axon branches crossing to the opposite side at the level of the tongue does not indicate that such an innervation does not exist because retrograde tracing studies in animals were not designed to address this problem, and no prior electrophysiological studies considered this question. In our data, nearly 50% of contralateral STAs resulted in identifiable potentials with predominantly delayed timing, suggesting contralateral representation at the level of the tongue. Given that crossing of muscle fibers is unlikely, our data can be best explained by the presence of motor axonal branches that cross the midline at the tongue level.

The delays of contralateral potentials from the trigger were typically 2.5–4.5 ms. This interval would include the conduction time in fine branches of motor axons, transmission delay in MEPs, and action potential conduction in muscle fibers. With the conduction distance in our study being about 6 mm transversely and 10 mm longitudinally, the net transmission velocity consistent with such a delay would be $<$2.6 m/s, which is less than transmission of action potentials in muscle fibers. This, in turn, suggests that the transmission velocity of action potentials in fine branches of motor axons that cross to the opposite side is considerably slower than in the main XII nerve motor axons as they exit the brainstem.

Recently, Trinder et al. (2013) reported that a common drive can be detected using coherence analysis in pairs of SMUs simultaneously recorded from the GG (innervated by the XII nerve) and tensor palatini (innervated by the trigeminal nerve) in humans. In particular, they found that common oscillations at frequencies $<$5 Hz were significantly stronger for SMU pairs recorded on the same side than on the opposite sides of the midline but nevertheless could be detected bilaterally. This appears to be analogous to our present findings. However, the correlations observed by Trinder et al. (2013) between GG and tensor palatini SMUs were strongest for SMU pairs with IT pattern of activity and weakest for SMUs with T activity, whereas our most prominent contralateral STA potentials were obtained with T SMUs. Indeed, the results reported by Trinder et al. (2013) are consistent with data from animal studies showing that respiratory-modulated motoneurons, even those innervated by different motor nerves and motor nuclei, receive a correlated high-frequency oscillation whose origin is in the central respiratory network (Peever and Duffin 2001; Rice et al. 2011; Tarras-Wahlberg et al. 2009). As such, this type of correlation is caused by a different mechanism than the short-latency and short-duration action potentials detected in the present study in relation to the triggering action potential. Specifically, when our contralateral STA potentials had a distinct time shift and amplitudes compatible with the amplitudes of the ipsilaterally recorded STA potentials, this could only be explained by the presence of some branches of motoneuronal axons crossing the midline and innervating muscles on both sides of the midline.

For some trigger potentials, we detected positive amplitude correlations among the STA potentials recorded at different sites. The observed pattern of positive and negative correlations was at least partially consistent with a predominantly A-P orientation of muscle fibers recorded contralateral to the trigger and with an increased probability of muscle fibers recorded at anterior locations to have A-P orientation compared with the fibers recorded at posterior locations. In other words, there might have been a subset of active muscle fibers present at posterior locations that covered only a limited length of the GG in A-P direction. For such fibers, their positive amplitude

correlations with signals recorded at the same level on the opposite side could have been attributable to electrotonic spread of the signal from the source. On the other hand, the strong positive correlation between amplitudes of the contralateral anterior and posterior STA potentials would be expected if most contralaterally recorded STA potentials were generated in bundles of muscle fibers that had an A-P orientation and were relatively loosely scattered within the transverse cross section of the base of the tongue.

Crossed motor innervation is most common for T motor units. An important finding was that both the likelihood of occurrence and amplitude of STA potentials varied as a function of the discharge pattern of the motor unit. The motor units with T discharge patterns produced ipsilateral and contralateral STA potentials with a similar probability, whereas the incidence of contralateral potentials was significantly lower than for the ipsilateral STAs for both I and E SMUs. In addition, the amplitudes of contralateral STA potentials were significantly larger for the T than I or E SMUs. The contralateral STA potentials obtained with I units had the lowest amplitudes of all three types (Fig. 4*C*). Notably, the contralateral STA potentials obtained with I SMUs also had significantly shorter durations than the contralateral STA potentials obtained with either E or T SMUs. Collectively, it is likely that a considerable proportion of the contralateral STA potentials obtained with I SMUs were generated by means of electrotonic spread from the opposite side, rather than as a result of genuine crossing of motor nerves to the opposite side. By contrast, the high incidence, large amplitudes, and relatively long durations of contralateral STA potentials obtained with T SMUs strongly point to the motor axons of T XII motoneurons having relatively extensive collaterals bilaterally.

Previous studies in humans have shown that I motor units respond differently to a number of stimuli that alter respiratory drive, such as sleep onset (Wilkinson et al. 2008), arousal from sleep (Wilkinson et al. 2010), and hypercapnia (Nicholas et al. 2010), compared with E or T motor units recorded from the base of the tongue. In the present study, we found that E and T SMUs somewhat differed in terms of the incidence of contralateral STA potentials and their amplitudes, but these two categories were still relatively similar to each other compared with I SMUs. Furthermore, our STA potential duration data suggested that contralateral STA potentials obtained with I units were generated in relatively compact and small bundles of muscle fibers compared with either T or E units. Thus our present results indicate that the differences between T/E, on the one hand, and I, on the other hand, motor units extend to the pattern of their motor innervation and motor unit structure within the base of the tongue. Figure 6 captures these differences, as deduced from our present results. Figure 6*A* applies to I and possibly some E SMUs motor units, of which a small fraction have crossed motor innervation and for which the number (mass) of muscle fibers receiving crossed innervation is likely much smaller than the mass of the muscle fibers of the same motor unit located on the side of the origin of motor innervation. In contrast, Fig. 6*B* is mainly representative of SMUs with T discharge patterns and shows that they have similar numbers of muscle fibers on both sides of the midline and that their individual muscle fibers are relatively loosely distributed within the base of the tongue.

Potential functional relevance of crossed motor innervation of the tongue. The mechanical benefit of the distribution of motor activation to the opposite side of the midline in the base of the tongue may be to stabilize the position of the tongue. This interpretation is supported by our finding that crossed motor innervation is particularly prominent for the T motor units. Such motor units may be particularly important for setting the baseline (neutral) position and stiffness of the tongue onto which specific phasic movements are then superimposed, including those related to the respiratory rhythm, vocalization, and swallowing. It seems plausible that the speed and precision of the specific tongue movements can be best achieved by uncrossed motor innervation, whereas a degree of crossed motor innervation may impart mechanical benefit by

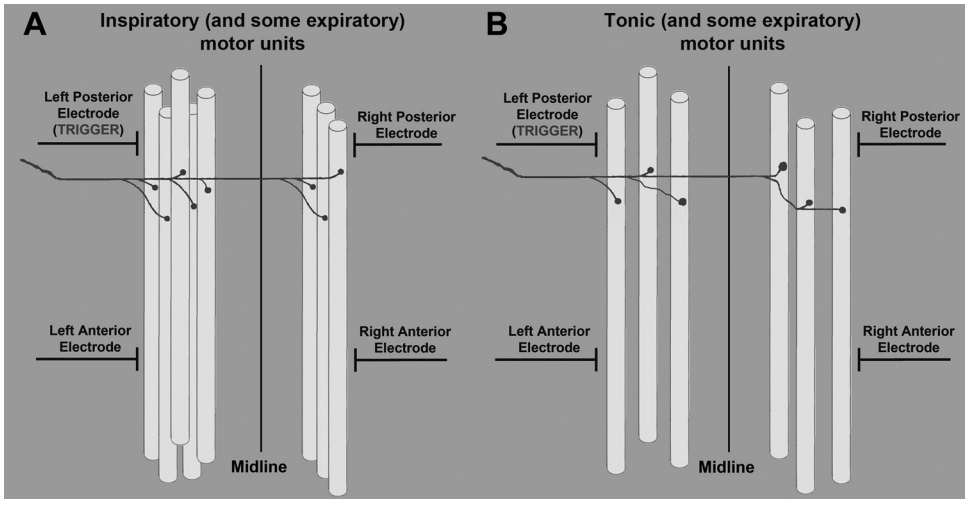

Fig. 6. Scheme of the prevailing neuromuscular connections between motor axons and their target muscle fibers within the horizontal compartment of the genioglossus in relation to the motor unit activity pattern, as supported by this study. *A*: scheme of the proposed innervation pattern and motor unit muscle bundle size and structure for inspiratory and some expiratory motor units. A relatively small fraction of these motor units had crossed motor innervation, and the number (mass) of muscle fibers located on the opposite side of the midline was smaller than the mass of the muscle fibers of the same motor unit located on the side of origin of motor innervation, as indicated by the large difference between the ipsilateral and contralateral STA potentials in favor of the former. *B*: in contrast to I motor units, for the T and a small fraction of E motor units, the intermediate and bilaterally similar amplitudes of STA potentials suggested that these motor units had similar numbers of muscle fibers on both sides of the midline, and their individual muscle fibers were relatively loosely distributed.

ensuring a stable static control of the baseline position of the tongue. The evidence that activity of T SMUs is independent of the central level of carbon dioxide and the level of central respiratory drive (Richardson and Bailey 2010) is consistent with such a scheme. If this interpretation is correct, it is possible that both the metabolic properties of the T muscle fibers and central connectivity of their motoneurons distinguish them from other motoneurons and their target muscles. This will need to be delineated in future studies.

Another potentially beneficial role of crossed motor innervation of the base of the tongue relates to conditions of neuromuscular injury, be it related to mechanical damage or degenerative changes. When motor innervation of the tongue or contraction of some of its muscle fibers is compromised, crossed motor innervation may help stabilize the position of the tongue. Crossed motor innervation may also facilitate the repair and regeneration of the motor innervation of the tongue following injury.

ACKNOWLEDGMENTS

L. Kubin was on a leave of absence from the Department of Animal Biology, School of Veterinary Medicine, University of Pennsylvania, Philadelphia, PA.

GRANTS

The study was supported by the Australian Research Council project grant DP120101343.

DISCLOSURES

No conflicts of interest, financial or otherwise, are declared by the authors.

AUTHOR CONTRIBUTIONS

Author contributions: L.K., A.S.J., C.L.N., J.M.C., J.G.S., and J.T. conception and design of research; L.K., A.S.J., C.L.N., J.M.C., J.G.S., and J.T. performed experiments; L.K., A.S.J., C.L.N., J.M.C., and J.T. analyzed data; L.K., A.S.J., C.L.N., J.M.C., J.G.S., and J.T. interpreted results of experiments; L.K., J.M.C., and J.T. prepared figures; L.K. and J.T. drafted manuscript; L.K., A.S.J., C.L.N., J.M.C., J.G.S., and J.T. edited and revised manuscript; L.K., A.S.J., C.L.N., J.M.C., J.G.S., and J.T. approved final version of manuscript.

REFERENCES

Abe S, Kikuchi R, Nakao T, Cho BH, Murakami G, Ide Y. Nerve terminal distribution in the human tongue intrinsic muscles: an immunohistochemical study using midterm fetuses. *Clin Anat* 25: 189–197, 2012.

Altschuler SM, Bao X, Miselis RR. Dendritic architecture of hypoglossal motoneurons projecting to extrinsic tongue musculature in the rat. *J Comp Neurol* 342: 538–550, 1994.

Arendt-Nielsen L, Zwarts M. Measurement of muscle fiber conduction velocity in humans: techniques and applications. *J Clin Neurophysiol* 6: 173–190, 1989.

Bailey EF. Activities of human genioglossus motor units. *Respir Physiol Neurobiol* 179: 14–22, 2011.

Dempsey JA, Veasey SC, Morgan BJ, O'Donnell CP. Pathophysiology of sleep apnea. *Physiol Rev* 90: 47–112, 2010.

Disselhorst-Klug C, Rau G, Schmeer A, Silny J. Non-invasive detection of the single motor unit action potential by averaging the spatial potential distribution triggered on a spatially filtered motor unit action potential. *J Electromyogr Kinesiol* 9: 67–72, 1999.

Doty RL, Cummins DL, Shibanova A, Sanders I, Mu L. Lingual distribution of the human glossopharyngeal nerve. *Acta Otolaryngol (Stockh)* 129: 52–56, 2009.

Eastwood PR, Allison GT, Shepard KL, Szollosi I, Hillman DR. Heterogenous activity of the human genioglossus muscle assessed by multiple bipolar fine wire electrodes. *J Appl Physiol* 94: 1849–1859, 2003.

Fregosi RF. Influence of tongue muscle contraction and dynamic airway pressure on velopharyngeal volume in the rat. *J Appl Physiol* 104: 682–693, 2008.

Fregosi RF, Ludlow CL. Activation of upper airway muscles during breathing and swallowing. *J Appl Physiol* 116: 291–301, 2014.

Horner RL, Hughes SW, Malhotra A. State-dependent and reflex drives to the upper airway: basic physiology with clinical implications. *J Appl Physiol* 116: 325–336, 2014.

Javaheri S, Redline S. Sleep, slow-wave sleep, and blood pressure. *Curr Hypertens Rep* 14: 442–448, 2012.

Jordan AS, White DP. Pharyngeal motor control and the pathogenesis of obstructive sleep apnea. *Respir Physiol Neurobiol* 160: 1–7, 2008.

Kairaitis K. Is the pharynx a muscular hydrostat? *Med Hypotheses* 74: 590–595, 2010.

Kezirian EJ, Goding GS Jr, Malhotra A, O'Donoghue FJ, Zammit G, Wheatley JR, Catcheside PG, Smith PL, Schwartz AR, Walsh JH, Maddison KJ, Claman DM, Huntley T, Park SY, Campbell MC, Palme CE, Iber C, Eastwood PR, Hillman DR, Barnes M. Hypoglossal nerve stimulation improves obstructive sleep apnea: 12-month outcomes. *J Sleep Res* 23: 77–83, 2014.

Kier WM, Smith KK. Tongues, tentacles, and trunks: the biomechanics of movement in muscular hydrostats. *Zool J Linn Soc* 83: 307–324, 1985.

Kubin L, Jordan AS, Nicholas CL, Cori JM, Semmler J, Trinder J. Divergent innervations and properties of human genioglossus and intrinsic muscle motor units in the tongue of healthy human subjects. *Sleep* 37: A35, 2014.

Lieberman DE, McCarthy RC, Hiiemae KM, Palmer JB. Ontogeny of postnatal hyoid and larynx descent in humans. *Arch Oral Biol* 46: 117–128, 2001.

Malhotra A, Trinder J, Fogel R, Stanchina M, Patel SR, Schory K, Kleverlaan D, White DP. Postural effects on pharyngeal protective reflex mechanisms. *Sleep* 27: 1105–1112, 2004.

Masuda T, De Luca CJ. Technique for detecting MUAP propagation from high-threshold motor units. *J Electromyogr Kinesiol* 11: 75–80, 1991.

McClung JR, Goldberg SJ. Functional anatomy of the hypoglossal innervated muscles of the rat tongue: a model for elongation and protrusion of the mammalian tongue. *Anat Rec* 260: 378–386, 2000.

McClung JR, Goldberg SJ. Organization of the hypoglossal motoneurons that innervate the horizontal and oblique components of the genioglossus muscle in the rat. *Brain Res* 950: 321–324, 2002.

McNicholas WT, Bonsigore MR. Sleep apnoeas an independent risk factor for cardiovascular disease: current evidence, basic mechanisms and research priorities. *Eur Respir J* 29: 156–178, 2007.

Mezzanotte WS, Tangel DJ, White DP. Waking genioglossal electromyogram in sleep apnea patients versus normal controls (a neuromuscular compensatory mechanism). *J Clin Invest* 89: 1571–1579, 1992.

Monster AW, Chan H. Surface electromyogram potentials of motor units; relationship between potential size and unit location in a large human skeletal muscle. *Exp Neurol* 67: 280–297, 1980.

Mu L, Sanders I. Neuromuscular organisation of the canine tongue. *Anat Rec* 256: 412–424, 1999.

Mu L, Sanders I. Neuromuscular specialization of pharyngeal dilator muscles: II. Compartmentalization of the canine genioglossus muscle. *Anat Rec* 260: 308–325, 2000.

Mu L, Sanders I. Human tongue neuroanatomy: nerve supply and motor endplates. *Clin Anat* 23: 777–791, 2010.

Newman AB, Nieto FJ, Guidry U, Lind BK, Redline S, Pickering TG, Quan SF, Sleep Heart Health Study Research Group. Relation of sleep-disordered breathing to cardiovascular disease risk factors: the Sleep Heart Health Study. *Am J Epidemiol* 154: 50–59, 2001.

Nicholas CL, Bei B, Worsnop C, Malhotra A, Jordan AS, Saboisky JP, Chan JKM, Duckworth E, White DP, Trinder J. Motor unit recruitment in human genioglossus muscle in response to hypercapnia. *Sleep* 33: 1529–1538, 2010.

Oliven A, Odeh M, Geitini L, Oliven R, Steinfeld U, Schwartz AR, Tov N. Effect of coactivation of tongue protrusor and retractor muscles on pharyngeal lumen and airflow in sleep apnea patients. *J Appl Physiol* 103: 1662–1668, 2007.

Patil SP, Schneider H, Schwartz AR, Smith PL. Adult obstructive sleep apnea: pathophysiology and diagnosis. *Chest* 132: 325–337, 2007.

Peever JH, Duffin L. Bilateral synchronisation of respiratory motor output in rats: adult versus neonatal in vitro preparations. *Pflügers Arch* 442: 943–951, 2001.

Remmers JE, de Groot WJ, Saurland EK, Anch AM. Pathogenesis of upper airway occlusion during sleep. *J Appl Physiol* 44: 931–938, 1978.

Rice A, Fuglevand AJ, Laine CM, Fregosi RF. Synchronization of presynaptic input to motor units of tongue, inspiratory intercostal, and diaphragm muscles. *J Neurophysiol* 105: 2330–2336, 2011.

Richardson PA, Bailey EF. Tonically discharging genioglossus motor units show no evidence of rate coding with hypercapnia. *J Neurophysiol* 103: 1315–1321, 2010.

Saboisky JP, Butler JE, Fogel RB, Taylor J, Trinder J, White DP, Gandevia S. Tonic and phasic respiratory drives to human genioglossus motor units during breathing. *J Neurophysiol* 95: 2213–2221, 2006.

Saboisky JP, Stashuk DW, Hamilton-Wright A, Carusona AL, Campana LM, Trinder J, Eckert DJ, Jordan AS, McSharry DG, White DP, Nandedkar S, David WS, Malhotra A. Neurogenic changes in the upper airway of patients with obstructive sleep apnea. *Am J Respir Crit Care Med* 185: 322–329, 2012.

Sanders I, Mu L. A three-dimensional atlas of human tongue muscles. *Anat Rec* 296: 1102–1114, 2013.

Sauerland EK, Harper RM. The human tongue during sleep: electromyographic activity of the genioglossus muscle. *Exp Neurol* 51: 160–170, 1976.

Suratt PM, McTier RF, Wilhoit SC. Upper airway muscle activation is augmented in patients with obstructive sleep apnea compared with that in normal subjects. *Am Rev Respir Dis* 137: 889–894, 1988.

Svanborg E. Impact of obstructive sleep apnea syndrome on upper airway respiratory muscles. *Respir Physiol Neurobiol* 147: 263–272, 2005.

Tarras-Wahlberg S, Rekling JC. Hypoglossal motor neurons in newborn mice receive respiratory drive from both sides of the medulla. *Neuroscience* 161: 259–268, 2009.

Trinder J, Woods M, Nicholas CL, Chan JKM, Jordan AS, Semmler JG. Motor unit activity in upper airway muscles genioglossus and tensor palatini. *Respir Physiol Neurobiol* 188: 362–369, 2013.

Wilkinson V, Malhotra A, Nicholas CL, Worsnop C, Jordan AS, Butler JE, Saboisky JP, Gandevia SC, White DP, Trinder J. Discharge patterns of human genioglossus motor units during sleep onset. *Sleep* 31: 525–533, 2008.

Wilkinson V, Malhotra A, Nicholas CL, Worsnop C, Jordan AS, Butler JE, Saboisky JP, Gandevia SC, White DP, Trinder J. Discharge patterns of human genioglossus motor units during arousal from sleep. *Sleep* 33: 379–388, 2010.

Young T, Finn L, Peppard PE, Szklo-Coxe M, Austin D, Nieto FJ, Stubbs R, Hla KM. Sleep disordered breathing and mortality: eighteen-year follow-up of the Wisconsin sleep cohort. *Sleep* 31: 1071–1078, 2008.

Zur KB, Mu L, Sanders I. Distribution pattern of the human lingual nerve. *Clin Anat* 17: 88–92, 2004.